Inorganic Nanotubes Stabilized by Ion Size Asymmetry: Energy Calculations for AgI Clusters

Adam Wootton and Peter Harrowell*

School of Chemistry, University of Sydney, Sydney, New South Wales 2006, Australia

Received: December 8, 2003; In Final Form: April 6, 2004

Using an accurate "rigid ion" potential for AgI developed by Parrinello, Rahman, and Vashishta, we have calculated the energy of AgI clusters containing up to 10^3 ions. Unlike the smaller halides such as Cl and Br, we find that the lowest energy clusters of AgI are trivalent polyhedral shells, instead of crystal fragments, for clusters up to around 100 ions. Most of these polyhedral minima take the form of nanotubes. We argue that the enhanced stability of such structures in AgI clusters arises from the same ion asymmetry that stabilizes the wurtzite structure in the bulk crystal.

1. Introduction

A variety of inorganic analogues of the fullerenes have been synthesized, inspired in some fashion by the original carbon compounds. Boron nitride, for example, is isoelectronic to the fullerenes and has been shown to generate stable nanotubes consisting of trivalent bonding between alternating N and B.[1] The stability of these BN clusters has received considerable theoretical attention.[2] Being isoelectronic with carbon represents a considerable constraint on potential candidates for "fullerine-like" clusters. As it turns out, this condition is not an essential requirement for the formation of nanotubes. The stability of carbon fullerenes can be regarded as arising from the competition between the edge energy of fragments of a graphite layer and the energy cost of bending the layer into a closed surface. This insight has motivated much of the search for inorganic fullerene-like materials[3] among other layer-forming compounds. MoS_2 and reduced oxides such as $H_2Ti_3O_7$ are two of the better studied examples of fullerine-like materials that exhibit layered structure in their bulk phases. Note that the layers here consist of multiple atomic layers.

In this paper we examine the zero temperature structures of neutral clusters of a 1:1 ion system in which the asymmetry of the ionic radii is large enough to destabilize the six-coordinated rock salt structure in favor of four-coordinated wurtzite. We present theoretical results that indicate an enhanced stability of nanotubes in clusters of ions that, in the bulk, occur as 1:1 ionic solids with tetrahedral structures.

The ground-state structures of ionic clusters have been the subject of a considerable number of theoretical studies. NaCl and KCl have been shown to form clusters dominated by the bulk rock salt structure[4−6] in classical calculations involving rigid ion models. Metastable minima corresponding to amorphous structure have been reported following simulations of rapid cooling of $(KCl)_{32}$.[5] Ahlrichs et al.[7,8] have performed extensive ab initio calculations on LiF, NaCl, and KCl. While confirming the stability of rock salt fragments for the latter two alkali halides, these calculations showed that LiF favors nanotubes based on stacking $(LiF)_3$ hexagons in the clusters with fewer than 27 ion pairs. Aguado et al.[9] have reported that the transition between stable rock salt fragments and stacked hexagonal rings in small alkalai halide clusters occurs when the ratio of the cation radius over the anion radius drops below 0.5. In larger clusters LiF also preferred bulklike geometries. Wilson,[10] using a polarizable ion model, has shown that MgO behaves similarly to LiF, forming nanotubes consisting of stacked hexagons in small clusters of less than 30 MgO pairs. Small clusters of $(NaI)_a$ with $a \leq 15$ have also been found to exhibit ground-state geometries that alternate between stacked hexagons and rock salt fragments as the number of ions change.[11,12] Theoretical calculations of other semiconductor materials, GaN[13] and ZnS,[14] have suggested that trivalent polyhedral structures are stable.

We show here that the lowest energy structures of silver iodide clusters of up to 10^2 ions are not fragments of the bulk crystal but, instead, trivalent polyhedra. To compare these clusters with those formed by materials with a more highly coordinated bulk crystal structure, we have also carried out calculations on AgBr clusters. We note that there is considerable interest in small crystallites of silver halides due to their application in photographic processes.[15] The growth mechanism of these materials is of considerable interest with regard to the control of size distribution in silver halide colloids[16] and in the photochemical generation of silver clusters.[17]

The paper is organized as follows. In the following section we describe the ion potential used in this study along with our approach to generating the various cluster structures. In Section 3 we present results for the minimum energy of AgI clusters and compare these with the lowest energies of clusters based on wurtzite and sphalerite. We argue that the enhanced stability of the polyhedral structures in AgI over AgBr arises from the same ion asymmetry that stabilizes sphalerite or wurtzite over rock salt in the bulk crystal. Some structural characteristics of the ground states of the AgI clusters are examined.

2. Model

2.1. Ionic Potentials. Parrinello, Rahman, and Vashishta[18] (PRV) have developed a pairwise "rigid ion" potential for AgI that has proven remarkably accurate in its prediction of the phase behavior of this material. The equations for the PRV interaction potentials are (with energy in units of electronvolts and distance in angstroms)

10.1021/jp037760r CCC: $27.50
Published on Web 05/22/2004

$$V_{AgAg}(r) = \frac{0.014804}{r^{11}} + \frac{0.36}{r} \quad (1)$$

$$V_{AgI}(r) = \frac{114.48}{r^{9}} - \frac{0.36}{r} - \frac{1.1736}{r^{4}} \quad (2)$$

$$V_{II}(r) = \frac{446.64}{r^{7}} + \frac{0.36}{r} - \frac{2.3472}{r^{4}} - \frac{6.9331}{r^{6}} \quad (3)$$

The model system undergoes a transition from a wurtzite structure to body centered cubic (bcc) at a temperature of 484 ± 12 K according to PRV[18] and approximately 420 K according to Tallon.[19] Madden et al.[20] have suggested that this difference in transition temperatures may reflect differences in system size and the long-range pressure corrections. The experimental value of this transition temperature is 420 K. While the PRV potential has not been generalized to other choices of halides, we would like to examine how the stability of the polyhedra varies with anion size. Born−Mayer−Huggins (BMH) potentials are available for AgBr[21] with the following mathematical form,

$$\phi_{ij}(r) = A_{ij}\exp(-r/\rho_{ij}) - \frac{B_{ij}}{r^{6}} + C\frac{q_i q_j}{r} \quad (4)$$

with $C = 14.399862e^{-2}$ eV Å, where e is the electron charge. The values of the other interaction parameters for AgBr are provided in Table 1. Given the relatively small number of particles used in the clusters no truncation of the potential has been used and the Ewald summation of the Coulomb interactions is not required.

While the PRV potential accurately reproduces much of the energetics of bulk AgI, it has not, to our knowledge, been used before in AgI clusters. To check the validity of the potential under these conditions we have carried out the following series of quantum calculations. We selected the three lowest energy $n = 24$ clusters as identified using the PRV potential. Using the minimum energy structure of each as a starting point, we then carried out geometry optimizations at the Hartree−Fock (HF) level. The Stuttgart−Dresden relativistic effective core potentials and SDD valence basis of Stoll et al.[22] are used, whereby a [6s,5p,3d] contracted Gaussian basis is utilized to accommodate the 4s, 4p, 4d, 5s electrons (19) of Ag and the [2s,3p] basis for the 5s, 5p valence electrons (7) of I. The energy of the structure generated by the Hartree−Fock procedure was recalculated with the Density Functional Theory utilizing the B3LYP hybrid density functional[23] to estimate the energetic contributions of electron correlation. The HF and B3LYP calculations were carried out with Gaussian98[24] on DEC alpha 600/5/333 and COMPAQ XP1000/500 workstations of the Theoretical Chemistry group at the University of Sydney.

In Table 2 we have compared the cluster energies, relative to the lowest energy cluster (identified here as "cluster 1"), as determined by the PRV potentials, the HF, and the B3LYP calculations. We find, first, that the order of clusters in terms of increasing energy is correctly reproduced by the PRV potentials. Second, the PRV potentials also manage to reproduce the magnitude of the energy differences between clusters to quite reasonable accuracy, with a maximum relative error of only 10% between the PRV and density functional values.

The dependence of the structure of the clusters on the method of energy minimization has also been examined. We have calculated the mean squared difference $\langle\Delta\Theta^2\rangle$ between bond angles and the mean squared difference $\langle\Delta d^2\rangle$ between bond lengths in the structures obtained from the PRV model and the HF calculation. The relative magnitudes of these average differences, i.e., $\langle\Delta\Theta^2\rangle^{1/2}/\langle\Theta\rangle$ and $\langle\Delta d^2\rangle/\langle d\rangle$ with $\langle\Theta\rangle$ and $\langle d\rangle$ being the average bond angle and bond length from the PRV model, are presented in Table 2. We find very little change in bond angles and hence cluster geometry between the PRV and HF calculations. While the bond lengths in the lowest energy cluster are very similar, we did observe a systematic increase in the bond length of about 12% in the HF calculations as compared with the PRV model in the two higher energy clusters. One possible cause for this expansion in the lower symmetry clusters is polarization of the anions. We conclude that the PRV potentials provide a reasonably accurate estimate of the relative energies between AgI clusters and the structures of these clusters.

TABLE 1: The BMH Parameters for the AgBr Interactions

	A (eV)	ρ (Å)	B (eV Å^6)
AgBr	3037.0	0.3234	228.39
BrBr	2948.2	0.3320	124.7
AgAg	16528.0	0.2310	2224.0

TABLE 2: A Comparison of the Energies and Structures of Three Lowest Energy $n = 24$ Clusters As Calculated by Using the PRV Potentials and Two Levels of Quantum Calculations As Described in the Text[a]

	E(cluster n) − E(cluster 1)				
	PRV (eV)	HF (eV)	B3LYP (eV)	$\langle\Delta\Theta^2\rangle^{1/2}/\langle\Theta\rangle$	$\langle\Delta d^2\rangle^{1/2}/\langle d\rangle$
cluster 1	0	0	0	0.0074	0.0287
cluster 2	0.4849	0.4627	0.5362	0.0170	0.1200
cluster 3	0.7161	0.5825	0.6805	0.0180	0.1200

[a] The energies are presented relative to the energy of the most stable cluster, labeled as 1. For each cluster the relative rms difference in bond angles Θ and bond lengths d between the minimum energy structure obtained by using the PRV potentials and the analogous structure obtained from the HF calculation is presented.

2.2. Generation of Structures. Unlike the approach of refs 5 and 6, we have made no attempt to sample over the entire configuration space of the clusters. Our limited aim is to compare the stability of polyhedra with that of the lowest energy fragments of the bulk crystal. The polyhedra were generated with a program called CaGe, developed at Uni-Bielfield,[25] that generates all possible trivalent polyhedra with a given number of vertexes and within the specified range of numbers of specific types of faces. The requirement that only anion−cation neighbors occur results in restricting the faces to be even sided. This means that the pentagon, which plays such a crucial role in generating curvature in the fullerenes, is absent here. Curvature in these inorganic polyhedra results, instead, from the presence of squares.[2] Applying Euler's formula,[26] we find the following relations between the number of faces with i edges and n number of vertexes, f_i,

$$n = 8 + 2f_6 + 4f_8 \quad (5)$$

$$f_4 = 6 + f_8 \quad (6)$$

when only 4-, 6-, and 8-sided faces are considered. Note that six is the minimum number of square faces possible. We have generated all possible polyhedra consisting of 4-, 6-, and 8-sided faces for the number of ions $n \leq 30$. For clusters larger than this, the number of possible structures increases rapidly and some extra topological restriction of the selected clusters was necessary to keep the number of clusters manageable. Examining the lowest energy cluster for each value of n up to 30 we found that none included an 8-sided face. On this basis, we exclude such faces from the clusters with $30 \leq n \leq 48$. This restriction

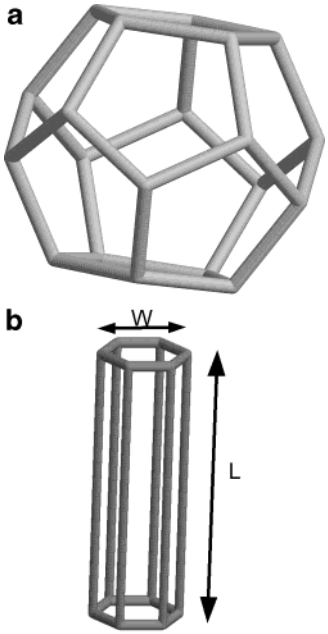

Figure 1. (a) Diagram of the regular dodecahedron cluster shape used for sphalerite structure. (b) Diagram of a wurtzite cluster bounded by the six $(11\bar{2}0)$ planes and capped top and bottom by the (1000) basal planes. The length L and width W are indicated.

means that we are only considering clusters with the minimum number of square faces. Once we reach $n = 48$, even this restricted space of clusters is becoming very large. As tube-like clusters dominate the minimum energy structures in the range $30 \leq n \leq 48$, we consider only such tubes in calculating minimum cluster energies for $n > 48$. The structure of these tubes is described in some detail in the following section. While a nanotube cluster may not be the true minimum energy structure for a given cluster size, we argue that these tube-like clusters are close enough to the true ground state to provide a reasonable measure of the trend in the cluster energy minimum as the number of ions increases.

Having generated each polyhedral net, we have two choices of how to fill the sites with anions and cations. We have examined each polyhedron with regard to whether its energy minimum changes or not with the global exchange of cation with anion. In addition to being a necessary consideration in locating the global energy minimum for a particular polyhedral arrangement, the change in minimum energy of a given structure with respect to inversion of the cations and anions could prove to be a useful symmetry.

We also have to generate clusters consisting of fragments of bulk crystal structures. The most stable forms of such clusters will be those with the lowest energy crystal surfaces. Where possible, this means identifying the charge neutral planes. In the case of the rock salt structure, these are the (001) surfaces. These surfaces produce clusters based on rectangular prisms. At each cluster size we have generated a number of possible arrangements of the rock salt unit cells chosen to minimize the surface area. The (011) plane of the sphalerite structure is also charge neutral. The cluster that exposes only these surfaces is the regular dodecahedron (see Figure 1a). The regularity of this shape restricts the number of ions n to a discrete sequence, the first three members are $n = 40$, 88, and 184.

Wurtzite, in contrast to sphalerite, is a hexagonal structure with only the six $(11\bar{2}0)$ hexagonal faces charge neutral. As indicated in Figure 1b, these faces are insufficient to enclose a cluster and additional charged surfaces must be used. The somewhat arbitrary choice of these additional bounding planes is reflected in the indeterminacy of the observed crystal forms of the mineral wurtzite. We have used a basel plane (1000) to generate hexagonal prisms. Hamad et al.[27] have examined the stable crystal morphologies of ZnS based on a potential fitted to density functional results. In the case of the wurtzite structure, they have found that the inclusion of the $(10\bar{1}0)$ faces, lying between the $(11\bar{2}0)$ faces, leads to a lower crystal energy. As we shall only go up to clusters containing 1000 ions in this paper, we have omitted these extra surfaces. Each such prism can be characterized by a length L and a width W in units of cell dimensions, as indicated in Figure 1b. We have calculated the energy minima using all combinations of L and W consistent with the range of ion number n. The cluster energies presented represent the lowest energy envelope of these various families of hexagonal clusters.

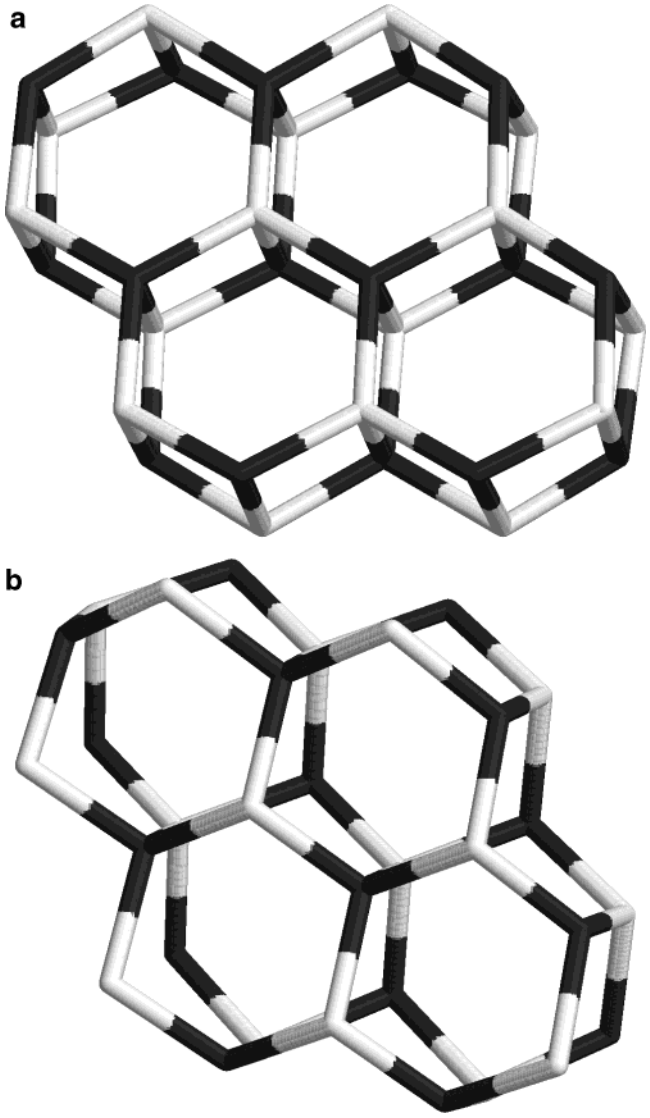

Figure 2. (a) A "flattened wurtzite" cluster consisting of 32 ions. (b) A wurtzite cluster of the same size. Note the higher coordination of the edge ions in part a, the flattened structure.

We have also considered a modification of the wurtzite cluster in which the chair rings of the basel plane are flattened. While this change increases the energy of the rings, it allows for higher coordination about the edges, as shown in Figure 2. These structures are referred to as "hexagonal stacks".

The potential energy of a cluster is minimized by using a conjugate gradient scheme.[28] To follow the aggregation of ions,

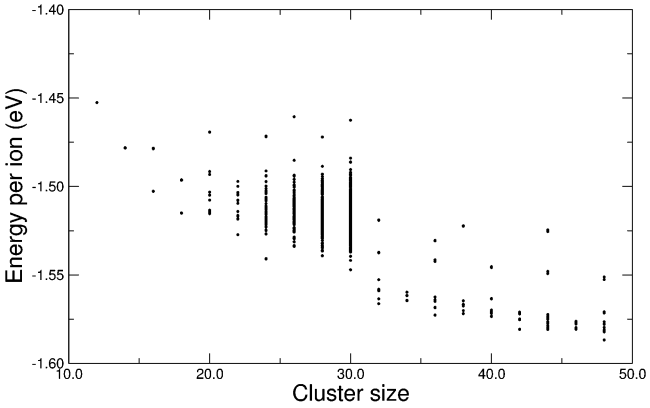

Figure 3. Scatter plot of the minimized cluster energies for all AgI polyhedral clusters generated as a function of *n*, the number of ions. Note the decrease in the number of clusters generated for $n \geq 32$ due to the neglect of 8-fold (and higher) faces.

the results of which are described in the following section, we have also carried out Monte Carlo (MC) runs using the Metropolis scheme.[29]

3. Results

3.1. Minimum Energy Structures of AgI Clusters. The minimum energy per particle for the polyhedral clusters of AgI (selected as described previously) for $n \leq 48$ are plotted in Figure 3. (The drop in cluster numbers for $n \geq 32$ is due to the neglect of 8-sided faces from this size on.) In Figure 4 we have plotted the lowest cluster energy for each value of *n* along with the analogous lowest energies for rock salt, sphalerite, wurtzite, and "flattened wurtzite" fragments. Diagrams of the structures of the lowest energy clusters for $12 \leq n \leq 48$ are provided in Figure 5. The minimum energy of these particular structures is invariant to the exchange of anions and cations.

There are "magic numbers" corresponding to particularly stable structures with substantial energy gaps between the lowest energy structure and the next lowest, at $n = 24$, 30, 32, 36, 42, and 48. For $n = 24$, the lowest energy structure is the truncated octahedron. One family of "magic number" clusters consists of nanotubes capped at either end by half of the truncated octahedron for which $n = 24 + 6m$ where $m = 0, 1, 2, \ldots$. An example of this class of nanotubes is shown in Figure 6, labeled as a (3,3) tube following the standard fullerene convention.[31] At $n = 48$ we find a new structure, more potato than tube, that has a lower energy than the (3,3) tube (which appears as the next-to-lowest energy structure). For $n > 48$ in Figure 4 we have assumed that the (3,3) tube will either be the minimum energy structure or, at least, be close enough in energy to this structure to provide a reasonable estimate of the lowest cluster energy. We note that there appears to be little in the way of an energy barrier to the end-to-end fusion of short (3,3) tubes to form longer ones. In contrast, there does not appear to be any "easy" path for fusion of two tubes side by side.

From Figure 4, we see that the stability of the polyhedral clusters of AgI over those based on the bulk crystal structure persists up to at least $n = 100$. Presumably, the low-coordinated surfaces of the bulk crystal fragments, along with the edges and corners, contribute to energy increases that are not adequately compensated by the relative stability of 4-coordination (in the bulk crystal structure) vs the 3-coordination of the polyhedra. The extended stability of the nanotubes suggests that it might be possible to observe them in AgI precipitates. The relative stability of the nanotubes also leaves open the question as to how does the bulk crystal finally form if it has to grow via these intermediate structures?

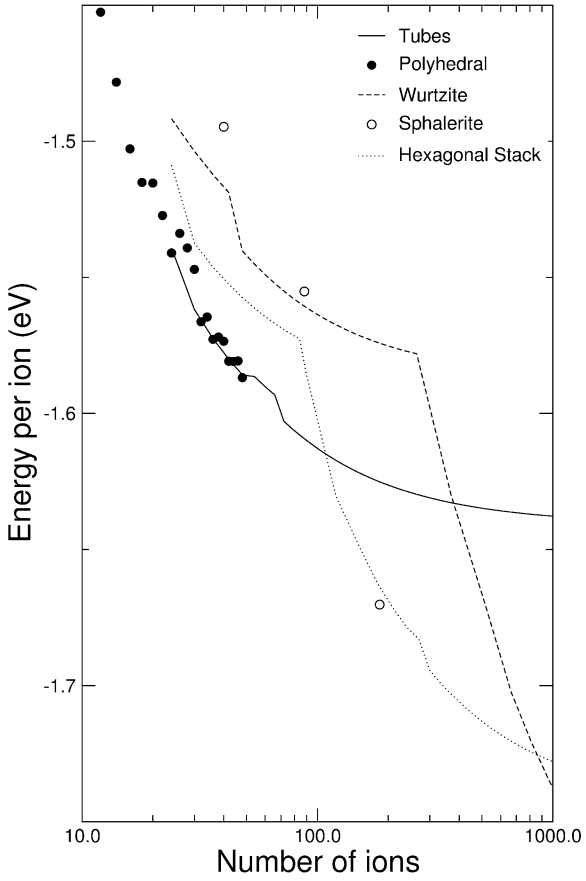

Figure 4. Plot of the minimum cluster energy for the polyhedral AgI clusters at each cluster size. These values are compared with the minimum energies of the clusters of rocksalt, sphalerite, wurtzite, and "hexagonal stack" clusters. The wurtzite cluster curve is the lower envelope of all combinations of the length *L* and width *W*.

The low-energy structures described here may not be kinetically very accessible. The very symmetry of some of the polyhedral cages would suggest that the mechanism by which they are formed must be considerably constrained. To explore this issue, we have allowed a cluster to form via a Monte Carlo process, one AgI pair at a time, at a temperature $T = 300$ K, until a cluster of 48 ions was reached. Each ion pair was allowed to find its place before the next pair was introduced at a random position on a spherical shell 20 Å from the center of mass of the growing cluster. This aggregation procedure was repeated 15 times to provide some statistics concerning the outcome of this growth process. We note that this specific protocol does not address the possible long-time relaxation processes. Given the strength of the ionic bonds, rearrangements involving bond-breaking are unlikely to be seen in any simulations at room temperature.

The results of the aggregation runs are as follows. (1) We have observed clusters of up to 30 ions aggregating into the perfect ground-state polyhedra. (2) For clusters larger than 24 ions, the average minimum energy of the aggregated structures deviates positively from the ground-state energies, as shown in Figure 7. For larger cluster sizes, we find the average energy of the aggregated cluster to be roughly 0.025 eV above that of the ground state. (3) This trend is mirrored structurally in the observed steady increase in the average fraction of ions with 4-fold coordination in clusters larger than 24 ions, as depicted in Figure 8. We conclude that while complete trivalent polyhedra *can* form via a stepwise aggregation, their probability of doing so drops off dramatically once the number of ions exceeds 24.

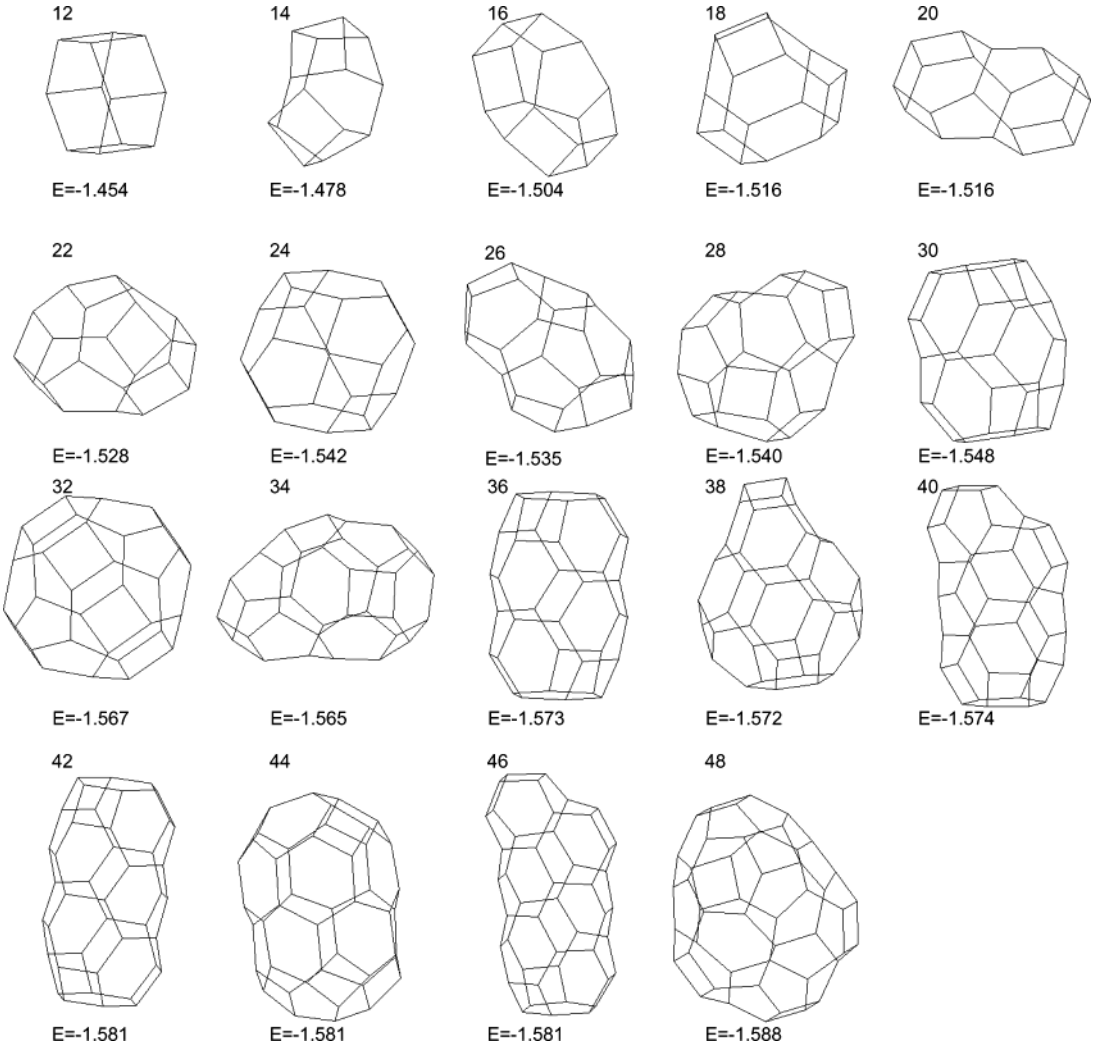

Figure 5. Diagrams of the lowest energy polyhedral clusters for AgI clusters with $n \leq 48$. Each structure is labeled by the number of ions and the minimum energy, the latter expressed in eV/ion.

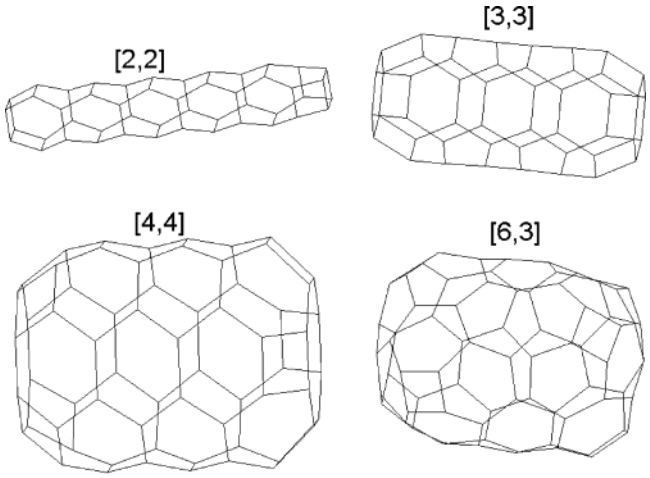

Figure 6. Diagrams of some possible tube-like structures presented to illustrate the labeling scheme described in ref 27.

The reason for this appears to be the very stability of the truncated octahedron ground state of the 24-ion cluster. This rather unavoidable intermediate in the growth process is not conducive to the formation of the larger trivalent structures. In the run in which the $n = 30$ ground-state cluster was achieved, the 24-ion ground state was avoided. We again remind the reader that this discussion refers only to the short-time dynamics accessible to room temperature simulation. It is possible that over much longer times, some these aggregated clusters will relax to the ground states.

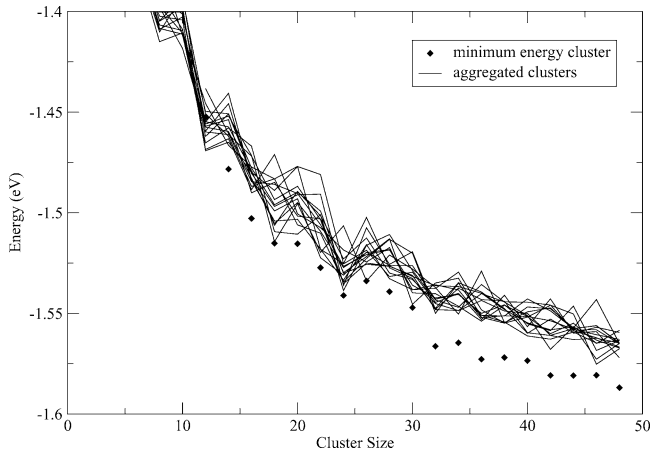

Figure 7. The 15 sequences of cluster energies (solid lines) generated by the random aggregation process described in the text. The energy of each cluster reflects its local minimum following conjugate gradient minimization. The minimum cluster energy at each value of the number of ions n is represented as a filled circle.

3.2. Rules Governing the Extended Stability of Polyhedral Clusters. To understand the role of the ion potential in determining cluster structure, we have carried out cluster energy calculations, analogous to those described for AgI, for clusters

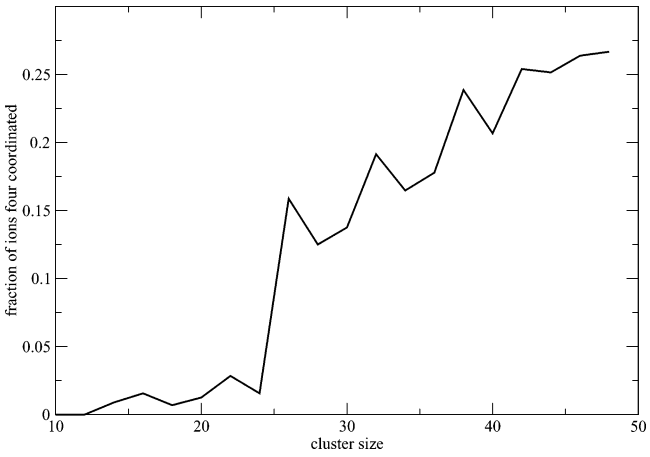

Figure 8. The fraction of four coordinated ions, averaged over the 15 separate aggregation runs, as a function of the number of ions *n*.

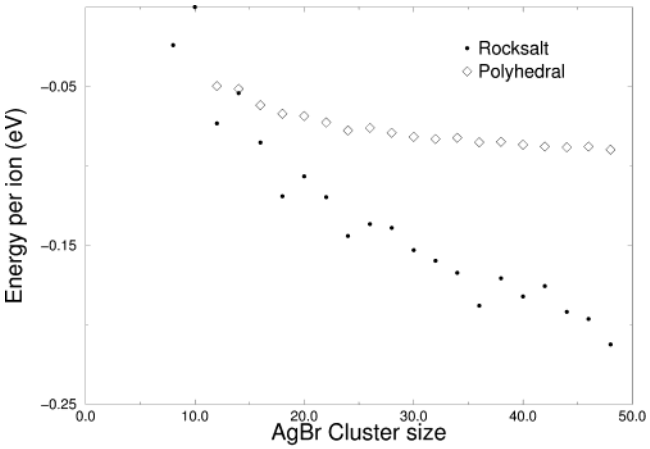

Figure 9. The minimum polyhedral cluster energies for AgBr compared with those of rock salt fragments.

of AgBr. The comparisons of the lowest energy trivalent cluster with that of the rock salt cluster are presented in Figure 9. In sharp contrast to the AgI results (and in agreement with previous studies[4−6]), we find that the crystal fragments are significantly more stable than the polyhedra for essentially all cluster sizes.

The extended stability of polyhedral clusters reported here for the AgI system appears to be closely linked to the destabilization of the rock salt structure. In an argument found in most standard texts[30] on ionic solids, hard sphere ions undergo a crossover in stability from rock salt to sphalerite when the ratio of anion to cation diameter exceeds 2.44. This transition can be understood by considering the stability of an elementary component of the rock salt structure, a pair of adjacent squares. As the anion radius grows, their repulsion across the square's diagonal forces the anion−cation separation to increase. Eventually, this energy increase becomes sufficient to force the squares to open to produce a buckled hexagon (chair configuration) as shown in Figure 10. Stacks of these buckled hexagons make up the wurtzite and sphalerite structures as well as the polyhedra described in this paper. While we have only demonstrated the stability of large nanotubes in the case of AgI, we believe that the general rationale for the stability of the polyhedral clusters could extend to include any ion system that forms a tetrahedral structure in the bulk. We note that this argument is similar to that put forward in ref 9 to account for the change in stability in alkali halide clusters from rock salt to stacked hexagons with increasing anion size relative to the cation.

Our arguments linking the instability of adjacent squares with the stability of polyhedra suggest two likely features of low-

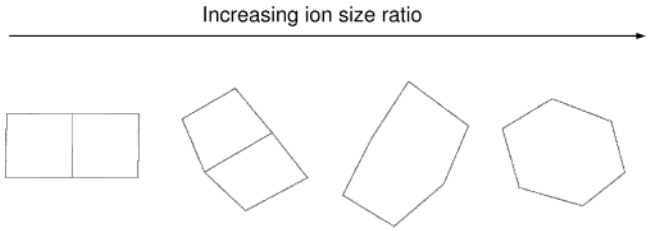

Figure 10. A sketch showing the transition between adjacent squares and buckled hexagon that results with increasing ratio of anion to cation size.

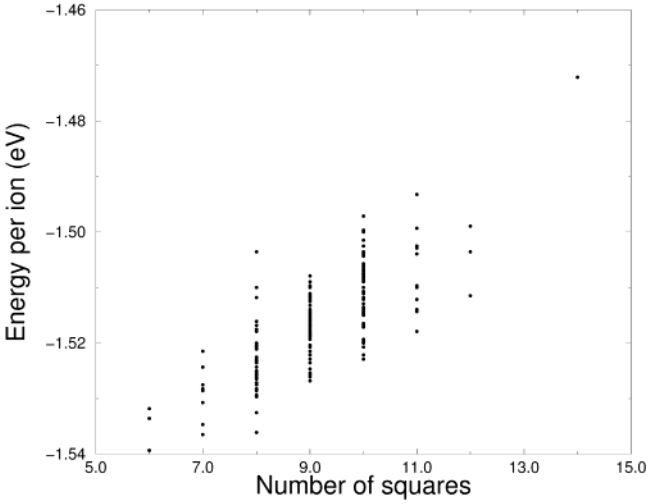

Figure 11. The scatter plot of the minimum cluster energy vs number of squares in polyhedral clusters consisting of 28 ions.

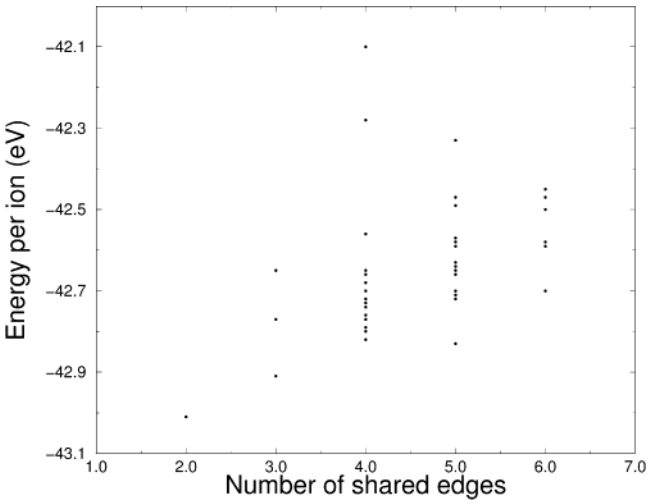

Figure 12. The scatter plot of the minimum cluster energy vs number of edges shared between squares in polyhedral clusters consisting of 28 ions with 8 squares.

energy polyhedra. These are that (a) the most stable polyhedra would have the minimum number of squares required by topology (i.e., six) and that (b) the number of edges shared between squares should be minimized, subject to the topological constraints of the given cluster. Condition a is found to apply in all the minimum energy clusters studied with $n < 32$. (We remind the reader that, for larger clusters, we have considered only those with the minimum number of squares.) In Figure 11 we have plotted the energies of all the clusters generated for 28 ions plotted against the number of squares. We find a general correlation between low square numbers and low energy. With regards to condition b, a glance through the structures sketched in Figure 5 reveals 13 of the 19 clusters involving squares

sharing edges. Over the similar range of cluster sizes in boron nitride, Fowler and co-workers[2] found only 8 clusters with associating squares. In Figure 12 we have plotted the minimum energies of all the possible polyhedral clusters consisting of 14 AgI ion pairs and 8 squares as a function of the number of edges shared between squares. There is a clear trend between low-energy structures and low numbers of shared edges, but strong fluctuations about this trend are also observed.

4. Conclusion

We have presented calculations of the potential energy of AgI clusters at zero temperature in which trivalent polyhedral structures represent the global minimum in clusters of up to roughly 100 ions. Among these polyhedral ground states, we have found examples of binary nanotubes. For larger AgI clusters, the ground states are either sphalerite fragments or hexagonal stacks. Given the stability of wurtzite in the bulk AgI using the PRV potentials,[18,19] we assume that a crossover to the wurtzite structure occurs for some cluster size larger that $n = 10^3$. While polyhedra have been found to be the minimum energy structure in ionic clusters previously, this was observed only for small clusters. The low-energy (3,3) nanotube consisting of 102 ions has dimensions of 37 Å by 7.6 Å. Such large asymmetric clusters may be observable—either directly through electron microscopy or through the influence of structure on electronic spectra.

We have proposed that the enhanced stability of the fullerene-like polyhedra in AgI arises from the same ion size asymmetry that stabilzes the wurtzite structure over the rock salt structure in the bulk. The significant difference in stability reported here between the polyhedral clusters of AgBr and those of AgI supports this general rule. Elsewhere we report on the analogous stability of polyhedral clusters of charged hard sphere mixtures.[32] We conclude that clusters of compounds that, in the bulk, form tetrahedrally coordinated structures are likely to exhibit these fullerene-like structures.

Acknowledgment. We gratefully acknowledge George Bacskay's assistance in carrying out the quantum calculations and helpful discussions with Paul Madden, Mark Wilson, and David Manolopoulos. This work has been supported by a Henry Bertie and Florence Mabel Gritton Research Scholarship.

References and Notes

(1) Chopra, N.; Luyken, R.; Cherrey, K.; Crespi, V.; Cohen, M.; Louie, S.; Zettl, A. *Science* **1995**, *269*, 966.

(2) Fowler, P.; Heine, T.; Mitchell, D.; Schmidt, R.; Seifert, G. *J. Chem. Soc., Faraday Trans.* **1996**, *92*, 2197.

(3) Tenne, R. *Chem. Eur. J.* **2002**, *8*, 5297.

(4) Martin, T. P. *Phys. Rep.* **1983**, *95*, 167.

(5) Rose, J.; Berry, R. S. *J. Chem. Phys.* **1993**, *98*, 3246. Rose, J.; Berry, R. S. *J. Chem. Phys.* **1993**, *98*, 3262.

(6) Doye, J.; Wales, D. *Phys. Rev. B* **1999**, *59*, 2292.

(7) Ahlrichs, R.; Ochsenfeld, C. *Ber. Bunsen-Ges.* **1992**, *96*, 1287.

(8) Ochsenfeld, C.; Ahlrichs, R. *Ber. Bunsen-Ges.* **1994**, *98*, 34.

(9) Aguado, A.; Ayuela, A.; Lopezm J.; Alonsom J. *Phys. Rev. B* **1997**, *56*, 15353.

(10) Wilson, M. *J. Phys. Chem.* **1997**, *101*, 4917.

(11) Diefenbach, J.; Martin, T. P. *J. Chem. Phys.* **1985**, *83*, 4585.

(12) Aguado, A.; Ayuela, A.; Lopez, J.; Alonso, J. *J. Phys. Chem. B* **1997**, *101*, 5944.

(13) Lee, S.; Lee, Y.; Hwang, Y.; Elsner, J.; Porezag, D.; Frauenheim, T. *Phys. Rev. B* **1999**, *60*, 7788.

(14) Spano, E.; Hamad, S.; Catlow, C. *J. Phys. Chem. B* **2003**, *107*, 10337.

(15) Eachus, R.; Marchetti, A.; Muenter, A. *Annu. Rev. Phys. Chem.* **1999**, *50*, 117.

(16) Hayes, D.; Schmidt, K.; Meissel, D. *J. Phys. Chem.* **1989**, *93*, 6100.

(17) Mulvaney, P. *Colloids Surf. A* **1993**, *81*, 231.

(18) Parrinello, M.; Rahman, A.; Vashishta, P. *Phys. Rev. Lett.* **1983**, *50*, 1073.

(19) Tallon, J. *Phys. Rev. B* **1987** 36, 776. Tallon, J. *Solid State Ionics* **1988**, *28*−*30*, 53.

(20) Madden, P.; O'Sullivan, F.; Chiarotti, G. *Phys. Rev. B* **1992**, *45*, 10206.

(21) Catlow, C.; Corish, J.; Harding, J.; Jacobs, P. *Philos. Mag. A* **1987**, *55*, 481.

(22) Andrae, D.; Hussermann, U.; Dolg, M.; Stoll, H.; Preuss, H. *Theor. Chim. Acta* **1990**, *77*, 123.

(23) Becke, A. D. *J. Chem. Phys.* **1993**, *98*, 5648. Becke, A. D. *Phys. Rev. A* **1988**, *38*, 3098. Lee, C.; Yang, W.; Parr, R. G. *Phys. Rev. B* **1988**, *37*, 785.

(24) Frisch, M. J.; Trucks, G. W.; Schlegel, H. B.; Scuseria, G. E.; Robb, M. A.; Cheeseman, J. R.; Zakrzewski, V. G.; Montgomery, J. A., Jr.; Stratmann, R. E.; Burant, J. C.; Dapprich, S.; Millam, J. M.; Daniels, A. D.; Kudin, K. N.; Strain, M. C.; Farkas, O.; Tomasi, J.; Barone, V.; Cossi, M.; Cammi, R.; Mennucci, B.; Pomelli, C.; Adamo, C.; Clifford, S.; Ochterski, J.; Petersson, G. A.; Ayala, P. Y.; Cui, Q.; Morokuma, K.; Malick, D. K.; Rabuck, A. D.; Raghavachari, K.; Foresman, J. B.; Cioslowski, J.; Ortiz, J. V.; Stefanov, B. B.; Liu, G.; Liashenko, A.; Piskorz, P.; Komaromi, I.; Gomperts, R.; Martin, R. L.; Fox, D. J.; Keith, T.; Al-Laham, M. A.; Peng, C. Y.; Nanayakkara, A.; Gonzalez, C.; Challacombe, M.; Gill, P. M. W.; Johnson, B. G.; Chen, W.; Wong, M. W.; Andres, J. L.; Head-Gordon, M.; Replogle, E. S.; Pople, J. A. Gaussian 98, revision A.7; Gaussian, Inc.: Pittsburgh, PA, 1998.

(25) The CaGe software was developed in the Department of Mathematics at the University of Bielefeld. At the time of this writing; the software is available from http://www.mathematik.uni-bielefeld.de/CaGe/Archive/.

(26) Cromwell, P. *Polyhedra*; Cambridge University Press: Cambridge, UK, 1997.

(27) Hamad, S.; Cristol, S.; Catlow, C. *J. Phys. Chem. B* **2002**, *106*, 11002.

(28) Press, W. H.; Teukolsky, S. A.; Vetterling, W. T.; Flannery, B. P. *Numerical Recipes in Fortran*; Cambridge University Press: New York, 1992.

(29) Allen, M. P.; Tildesley, D. J. *Computer simulation of liquids*; Oxford University Press: Oxford, UK, 1987.

(30) Cotton, F. A.; Wilkinson, G. *Advanced Inorganic Chemistry*, 3rd ed.; John Wiley: New York, 1972; p 53.

(31) Taylor, R. *Lecture notes on fullerene chemistry*; Imperial College Press: Cambridge, UK, 1999.

(32) Wootton, A.; Harrowell, P. In preparation.